

Spectral dimension and dynamics for Harper's equation

Michael Wilkinson^{*†} and Elizabeth J. Austin^{*†}

Department of Physics, Technion-Israel Institute of Technology, Haifa 3200, Israel

(Received 27 December 1993)

The spectrum of Harper's equation (a model for Bloch electrons in a magnetic field) is a fractal Cantor set if the ratio β of the area of a unit cell to that of a flux quantum is not a rational number. It has been conjectured that the second moment of an initially localized wave packet has a power-law growth of the form $\langle x^2 \rangle \sim t^{2D_0}$, where D_0 is the box-counting dimension of the spectrum, and that $D_0 = \frac{1}{2}$. We present numerical results on the dimension of the spectrum and the spread of a wave packet indicating that these relationships are at best approximate. We also present heuristic arguments suggesting that there should be no general relationships between the dimension and the spread of a wave packet.

I. INTRODUCTION

Harper's equation

$$\psi_{n+1} + \psi_{n-1} + 2 \cos(2\pi\beta n + \theta)\psi_n = E\psi_n \quad (1.1)$$

is a discrete Schrödinger equation, which can be thought of as describing the dynamics of an electron hopping between sites labeled by the index n , with a periodic modulation of the site energies. The principal physical importance of Harper's equation is somewhat different: it occurs as a one-band model for an electron moving in a plane with a spatially periodic potential and a uniform magnetic field perpendicular to the plane.¹⁻⁴ When β is a rational number p/q , Bloch's theorem is applicable and there is a band spectrum with q nonoverlapping bands. When β is irrational, the spectrum is a fractal Cantor set, which can be characterized by a noninteger dimensionality D ; various possible definitions of D are discussed by Falconer.⁵

There is a body of literature⁶⁻¹⁰ concerning general relationships between the dimensionality of the spectrum and the dynamics of the corresponding Hamiltonian. If the wave packet is initially localized with $\psi_n = \delta_{n0}$ at time $t = 0$, the N th moment of the wave packet might be expected to grow algebraically with exponent γ_N

$$\langle x^N \rangle = \sum_{n=-\infty}^{\infty} |n^N| |\psi_n(t)|^2 \sim t^{\gamma_N}. \quad (1.2)$$

Guarneri^{6,7} has proved that if the second moment has power-law growth, the exponent satisfies the rigorous lower bound $\gamma_2 \geq 2\mathcal{D}_1$, where \mathcal{D}_1 is the information dimension of the spectral measure of the wave packet: we must refer the reader to the original papers for a precise and general statement of this result. It has been proposed⁸ that the actual growth rate of the second moment $\langle x^2 \rangle$ is determined by the box-counting dimension D_0 of the spectrum of the Hamiltonian: i.e., that (1.2) is valid and that $\gamma_2 = 2D_0$. A variety of numerical results and heuristic arguments have been published^{11,12,8} that

support the hypothesis that the box-counting fractal dimension of the spectrum is $D_0 = \frac{1}{2}$. It is not always clear whether this is an approximate statement, or whether it is true for almost all β .

If they are true, the hypotheses that $\gamma_2 = 2D_0$ and $D_0 = \frac{1}{2}$ would indicate a surprising degree of insensitivity to the number theoretical properties of β , and deserve careful scrutiny. In this paper, we report numerical results on both the dimension D_0 of the spectrum and the spread of an initially localized wave packet. We will show that both of these results are, at best, only approximately correct.

We also give some heuristic arguments, which are aimed at clarifying why these proposed relationships are approximately but not exactly correct, and under what circumstances they might be expected to break down entirely. For this discussion it will be useful to describe the number β by its continued fraction expansion

$$\beta = \frac{1}{n_1 + \frac{1}{n_2 + \frac{1}{n_3 + \dots}}} = [n_1, n_2, n_3, \dots]. \quad (1.3)$$

The hierarchical structure of the Cantor set spectrum is related to the continued fraction expansion: roughly speaking, the spectrum can be divided into n_1 bands, each of which divides into n_2 subbands, etc. This structure was analyzed by Azbel¹³ using a semiclassical approach, which was subsequently extended by Suslov¹⁴ and Wilkinson.¹⁵ The precise scheme for describing the splitting of the spectrum is somewhat more complex and was described empirically by Hofstadter¹⁶ and explained by Wilkinson.¹⁷ We will pay particular attention to the class of quadratic irrational numbers of the form $\beta = [n, n, n, \dots]$, for which the subdivision of the spectrum is closest to exact self-similarity. When n is large, these numbers approximate rationals very closely, and the semiclassical arguments in Ref. 15 can be applied.

For a given irrational number β it is always possible to find sequences of rationals p_k/q_k such that

$$|\beta - p_k/q_k| < C/q_k^\alpha \quad (1.4)$$

for arbitrarily large q_k , where α and C are constants. Quadratic irrational numbers and typical irrationals share the property that the largest possible exponent is $\alpha = 2$. Last¹⁸ has shown rigorously that, for a set of irrationals of zero measure with $\alpha \geq 4$, the Hausdorff dimension of the spectrum satisfies $D_H \leq \frac{1}{2}$.

In Sec. II, we discuss some further facts about the spectrum and describe a Cantor set which is a reasonable model for the spectrum of Harper's equation for the sequence of quadratic irrationals $\beta = [n, n, n, \dots]$. We find that the box-counting dimension of this model is less than one-half, and that it approaches zero in the limit $n \rightarrow \infty$. The method can be extended to a variety of more refined models. In Sec. III, we consider an alternative and somewhat simpler approximate method for estimating the dimension of these Cantor sets, which is applicable when the dimension is close to one-half.

In Sec. IV, we discuss the spread of the wave packet, and conjecture that for the same sequence of irrationals the growth exponent γ_2 is unity in the limit $n \rightarrow \infty$. The higher moments are predicted to have faster than diffusive growth.

We discuss our numerical results in Sec. V, including results for both the quadratic irrationals $\beta = [n, n, n, \dots]$ and generic irrational numbers. Our results for the quadratic irrationals provide strong evidence that the spread of the wave packet satisfies (1.2) and that the box-counting dimension exists. The results do not support the hypothesis that $\gamma_2 = 2D_0$, and they are consistent with the hypotheses that $D_0 \rightarrow 0$ and $\gamma_2 \rightarrow 1$ as $n \rightarrow \infty$, although the convergence is very slow. The higher exponents γ_N are qualitatively consistent with the predictions of Sec. IV. For typical irrationals we see evidence that γ_2 exists and is approximately unity. The convergence of the data on the fractal dimension for typical irrationals is poor, but the results are not inconsistent with the existence of a dimension D_0 that is slightly less than one-half.

II. MODEL CANTOR SETS FOR THE HARPER EQUATION SPECTRUM

In this section, we describe how to calculate the dimension of a class of Cantor sets which is a reasonable model for the spectrum of Harper's equation. Before describing the model Cantor set we survey some relevant facts about the spectrum, and discuss the definition of the dimension D_0 .

When β is the ratio of two integers, $\beta = p/q$ (where p, q are relatively prime), Bloch's theorem is applicable and the spectrum consists of q non-overlapping bands. Thouless^{19,20} has discovered a remarkable property of the total bandwidth S (the union of the spectrum over all values of Δ) at the critical point

$$\lim_{q \rightarrow \infty} qS \rightarrow \frac{32C}{\pi} = 9.32995\dots, \quad (2.1)$$

where C is Catalan's constant. Although Thouless's

derivation of this result is restricted to $\beta \ll 1$, this result appears to hold for all β : a partial explanation of this remarkable fact is given by Last and Wilkinson.²¹

The spectrum has continuity properties with respect to varying β , implying that the spectrum for rational β is a good approximation to an economical covering set for the spectrum with a nearby irrational β . Technically, the spectrum is Hölder continuous with exponent $\frac{1}{2}$.²²

There are a variety of definitions of the generalized dimension D .⁵ The most satisfactory and fundamental one is the Hausdorff dimension D_H , but this is usually difficult to calculate. It is usually easiest to calculate a box-counting dimension D_0 , which requires us to calculate the minimal number \mathcal{N} of intervals of length δ required to cover the spectrum. The box-counting dimension is then

$$D_0 = -\lim_{\delta \rightarrow 0} \frac{\log_e \mathcal{N}(\delta)}{\log_e \delta} \quad (2.2)$$

if this limit exists. In general $D_0 \geq D_H$, but for many examples of Cantor sets, these dimensions are equal.

Thouless's observation leads to a simple heuristic argument that suggests that the dimension of the spectrum is equal to one-half, which Thouless pointed out to one of us. We consider a sequence of rational approximants $\beta_i = p_i/q_i$ to an irrational β . The bands of the rational approximants are assumed to form an economical covering of the irrational spectrum. At the i th stage of this construction, there are q_i bands, and because of (2.1) the average width of these bands is $\delta \sim 1/q_i^2$. This suggests that $\mathcal{N}(\delta) = q_i \sim \delta^{-1/2}$, implying that $D_0 = \frac{1}{2}$.

This argument assumes that all of the bands of the rational spectra are of the same size. The semiclassical arguments discussed in Ref. 15 indicate that (at energies away from the classical separatrix) the bandwidths are of the form

$$\Delta E = \hbar\omega(E) \exp[-S(E)/2\pi\beta], \quad (2.3)$$

where $S(E)$ is $O(1)$ at the edges of the spectrum and approaches 0 at $E = 0$. In the limit $\beta \rightarrow 0$ the smallest bandwidths are exponentially smaller than the largest. From the arguments in Ref. 15, it is clear that this will be the case whenever the continued fraction expansion of β contains at least some large coefficients n_i . It is, therefore, desirable to refine this model to take into account the marked dispersion in the sizes of the bands.

We therefore consider the following more refined model for the spectrum of Harper's equation. It is a Cantor set, constructed using a generating set G consisting of n nonoverlapping intervals with lower limits $(i-1)/n$, $i = 1, \dots, n$ and widths $g_i = \epsilon^i$, where ϵ is a constant. The Cantor set is constructed iteratively, by replacing each interval with a linearly scaled and shifted version of the set G , i.e., the interval $I = [x_1, x_2]$ is replaced by the set of n intervals which are images of the intervals of G under the transformation $x \rightarrow x' = (x_2 - x_1)x + x_1$. The construction of this Cantor set is illustrated in Fig. 1.

After k iterations, there are n^k intervals, and the total measure of the set is



FIG. 1. Illustrating four stages of the construction of the model Cantor set for $n = 3$.

$$W = \left\{ \sum_{i=1}^n \epsilon^i \right\}^k. \quad (2.4)$$

This set is intended to model the spectrum of Harper's equation when

$$\beta = \underbrace{[n, n, \dots, n, n]}_{k \text{ coefficients}}, \quad (2.5)$$

which is a rational number $\beta_k = p_k/q_k$ with denominator $q_k \sim n^k$ for large n . We choose the value of ϵ such that $Wn^k = 1$, which is analogous to the Thouless property (2.1): this requires that ϵ should satisfy the equation

$$\frac{\epsilon(1 - \epsilon^n)}{1 - \epsilon} = \frac{1}{n}. \quad (2.6)$$

The limiting Cantor set generated by this construction is a reasonable model for the spectrum of Harper's equation when β is a quadratic irrational number with continued fraction coefficients $\beta = [n, n, n, \dots]$: there are n "bands," each of which divides into n subbands, etc. In accordance with the semiclassical description, the bands have a broad range of sizes, with the smallest band of size ϵ^n exponentially small in $n \sim 1/\beta$, in accordance with (2.3).

We now calculate the box-counting dimension of this set. To facilitate this, we construct the set in a slightly different way. Instead of subdividing each interval, so that at the k th stage there are n^k intervals, we only subdivide intervals which are of size ϵ^k . Let us introduce an inductive hypothesis, that at the k th stage of the construction no pair of intervals can be covered by an interval of length ϵ^k : this is clearly true for $k = 1$. At the k th stage of the construction we subdivide the $N_1^{(k)}$ intervals of size ϵ^k , and leave the rest of the set, consisting of $N_i^{(k)}$ intervals of size ϵ^{k+i-1} , $i = 2, \dots, n$, unaltered. Clearly the subintervals resulting from the division of the intervals of length ϵ^k have separation ϵ^{k+1} , and no pair of subintervals resulting from this process can be covered by a single interval of length ϵ^{k+1} . The inductive hypothesis is therefore true. The number of intervals of

length ϵ^k required to cover the set at the k th stage of its construction is, therefore,

$$\mathcal{N}_k = \sum_{i=1}^n N_i^{(k)} \quad (2.7)$$

and this number cannot decrease as the set is further subdivided. The number of intervals of size ϵ^{k+i-1} satisfies the recursion relations

$$N_i^{(k+1)} = N_1^{(k)} + N_{i+1}^{(k)}, \quad i = 1, \dots, n-1,$$

$$N_n^{(k+1)} = N_1^{(k)}. \quad (2.8)$$

This is a linear mapping, of the form $\mathbf{v}^{(k+1)} = \tilde{M}\mathbf{v}^{(k)}$, where $\mathbf{v}^{(k)}$ is an n dimensional vector formed from the $N_i^{(k)}$, and \tilde{M} is a square matrix. The general solution is of the form

$$\mathbf{v}^{(k)} = \tilde{M}^k \mathbf{v}^{(0)} = \sum_{j=1}^n \alpha_j \lambda_j^k \mathbf{x}_j, \quad (2.9)$$

where the λ_j are the eigenvalues of \tilde{M} in ascending order of magnitude, and the α_j are determined by the initial condition $N_i^{(1)} = 1$, $i = 1, \dots, n$. We assume that the coefficient α_n corresponding to the largest eigenvalue λ_n is nonzero. For large k the solution (2.9) is then dominated by the largest eigenvalue, so that

$$D_0 = \lim_{k \rightarrow \infty} \left[-\frac{\log_e \mathcal{N}_k}{\log_e \epsilon^k} \right] = -\frac{\log_e \lambda_n}{\log_e \epsilon}. \quad (2.10)$$

Because the number of covers $\mathcal{N}(\delta)$ of size δ is a monotonic function, we see that the box-counting dimension exists and is equal to

$$D_0 = -\frac{\log_e \lambda_n}{\log_e \epsilon}. \quad (2.11)$$

By inspection of (2.8), the eigenvalues λ satisfy the equation

$$\lambda^n - \lambda^{n-1} - \dots - \lambda^2 - \lambda - 1 = 0. \quad (2.12)$$

The largest real eigenvalue approaches two from below in the limit $n \rightarrow \infty$. The value of ϵ approaches $1/(n+1)$ in the limit $n \rightarrow \infty$. The dimension of this set is less than $\frac{1}{2}$ for all n , and approaches $\log_e 2 / \log_e n$ in the limit $n \rightarrow \infty$. This argument, therefore, suggests that the dimension of the spectrum should be less than one half for numbers of the class $\beta = [n, n, n, \dots]$, and that $D_0 \rightarrow 0$ in the limit $n \rightarrow \infty$.

We end this section by discussing two generalizations that could be applied to more refined models for the Harper equation spectrum.

One limitation of the model considered above is that the sizes of the bands of the generating set G are in a geometric progression. To give a more realistic model, it would be desirable to use the bands of the Harper spectrum for $\beta = 1/n$ as the bands of the generating set G , and there is no reason to expect that the sizes of these

bands form an exact geometric series. We can, however, consider a construction similar to that of Sec. II in which not every power of ϵ is represented in the set of n bands; this still gives a recursion relation analogous to (2.8) for the numbers of covering intervals. By taking the limit $\epsilon \rightarrow 1$, we can approximate the desired set of lengths g_i to arbitrary precision by writing $g_i \approx \epsilon^{\nu_i}$, where ν_i are suitably chosen (large) integers.

This method for calculating the dimension can also be extended to a Cantor set in which the number n of intervals at each stage of subdivision is a random number with a probability distribution $P(n)$. The continued fraction coefficients of a typical irrational number form a quasirandom sequence with probability distribution²³

$$P(n) = \frac{1}{\log_e 2} \log_e \frac{(n+1)^2}{n(n+2)}, \quad (2.13)$$

and such a Cantor set would be a reasonable model for the spectrum of Harper's equation for typical irrational β . In this case, (2.9) would contain the product of a sequence of k random matrices, and the largest eigenvalue λ_n would be replaced by the largest Lyapunov exponent. This suggests that a universal box-counting dimension should exist for almost all irrational values of β . One of us¹⁵ previously argued incorrectly that the box-counting dimension should be zero for typical irrationals. This semiclassical argument was based upon an estimate for the bandwidths of the form (2.3), and it is incorrect because it ignores the fact that the action $S(E)$ vanishes at one energy, leading to the existence of bands that are not exponentially narrow.

III. ALTERNATIVE METHOD FOR ESTIMATING THE DIMENSION

When we examine the numerical results on the spectrum in Sec. V it will become apparent that the dimension of the spectrum is very close to $\frac{1}{2}$ for $\beta = [n, n, n, \dots]$ with small values of n . For this reason we will consider in detail a model in which the sizes of the bands are similar to each other, leading to a dimension that is very nearly one half. We will show that, in this case, the dimension can be estimated from a single statistic characterizing the set of lengths g_i of the intervals of the generating set.

Consider the direct method of construction of the Cantor set, in which all intervals are subdivided regardless of their length. After $m \gg 1$ stages of this construction, it is clear that the n^m intervals will have a distribution of lengths that is approximately log-normal, because the length of a given interval is the product of a large number of g_i , and these can be combined without restriction. We will, therefore, assume that the number of intervals after m stages of the construction is \tilde{n}^m (where \tilde{n} need not necessarily be an integer), and that the number of intervals of size between $\exp(-k)$ and $\exp(-k + dk)$ is

$$N(k, m) dk \sim \tilde{n}^m P(k) dk,$$

$$P(k) = \sqrt{\frac{1}{2\pi\sigma^2}} \exp[-(k - \bar{k})^2/2\sigma^2]. \quad (3.1)$$

The mean and variance of the "probability" distribution $P(k)$ are clearly proportional to m : we will write

$$\bar{k} = \mu_0 + \mu_1 m, \quad \sigma^2 = \sigma_0^2 + \sigma_1^2 m. \quad (3.2)$$

We will assume that the number of intervals of length $\delta = \exp(-k)$ required to cover the set is

$$\mathcal{N} \sim c \sum_m N(k, m) \sim c \int dm N(k, m), \quad (3.3)$$

where c is a constant. This assumption is correct for the type of model considered in Sec II. The integrand in (3.3) falls away very steeply from the maximum value of the function, and we have

$$\log_e \mathcal{N} \sim \log_e N(k, m^*), \quad (3.4)$$

where m^* is the value of m for which $N(k, m)$ is a maximum. In the limit $k \rightarrow \infty$ the dependence of the pre-exponential factor of $P(k)$ on m can be neglected, and the equation for the maximum of $N(k, m)$ can be approximated as follows:

$$\frac{\partial \log_e N}{\partial m} = 0 \sim \log_e \tilde{n} + \frac{\mu_1(k - \mu_1 m)}{\sigma_1^2 m} + \frac{(k - \mu_1 m)^2}{2\sigma_1^2 m^2}. \quad (3.5)$$

Solving (3.5) for m^* , we find

$$m^* \sim \frac{k}{\sqrt{\mu_1^2 - 2\sigma_1^2 \log_e \tilde{n}}} \quad (3.6)$$

and the maximum value of $\log_e N$ is, therefore,

$$\log_e \mathcal{N} \sim \log_e N(k, m^*) \sim \frac{k}{\sigma_1^2} [\mu_1 - \sqrt{\mu_1^2 - 2\sigma_1^2 \log_e \tilde{n}}]. \quad (3.7)$$

The box-counting dimension is, therefore,

$$D_0 = \frac{-\log_e \mathcal{N}}{\log_e \delta} = \frac{1}{k} \log_e \mathcal{N} \sim \frac{1}{\sigma_1^2} [\mu_1 - \sqrt{\mu_1^2 - 2\sigma_1^2 \log_e \tilde{n}}]. \quad (3.8)$$

If we require that the sum of the widths of the intervals is $S = 1/n^m$, to simulate the Thouless property (2.1), the coefficients α_1 and β_1 will not be independent. The total width of the intervals at the m th stage of construction is

$$\begin{aligned} S &= \frac{1}{n^m} = \int d\delta \delta N(\delta, m) = \int dk e^{-k} N(k, m) \\ &\sim \frac{1}{\sqrt{2\pi\sigma^2}} \int dk \exp[-k - (k - \bar{k})^2/2\sigma^2] \\ &\sim \tilde{n}^m e^{-\bar{k}} e^{\sigma^2/2}. \end{aligned} \quad (3.9)$$

From (3.9) and (3.2), we find the following relationship between the coefficients μ_1 and σ_1^2 :

$$\mu_1 = 2 \log_e \tilde{n} + \frac{1}{2} \sigma_1^2. \quad (3.10)$$

Substituting this into (3.8), we find

$$D_0 \sim \frac{1}{2} - \frac{\sigma_1^2}{16 \log_e \bar{n}}. \quad (3.11)$$

It is difficult to extend this heuristic calculation to give an estimate for the errors of the approximations used. The most important source of error in this result is related to the assumption that the bandwidths are log-normal distributed. The log-normal approximation is valid close to the maximum of the distribution, but breaks down in the tails. This implies that the position of the maximum of the product $\bar{n}^m P(k)$, determined in (3.5), will be accurately determined only if the position of the maximum m^* is close to the maximum of the distribution $P(k)$. This condition will be satisfied if the dispersion coefficient σ_1^2 of the bandwidths is small. These considerations suggest that the error of (3.11) is probably $O(\sigma_1^4)$.

We illustrate the applicability of (3.11) by showing that it gives the correct result for a specific model in the limit $\sigma_1^2 \rightarrow 0$. We consider a model of the type considered in Sec. II, in which the lengths g_i are given by

$$g_i = \epsilon^{i+N}, \quad i = 1, \dots, n. \quad (3.12)$$

This reduces to the previous model when $N = 0$. Our interest will be in the dimension of this model when $N \gg n$, in which case the dispersion in the lengths of the intervals is very small. By a simple adaptation of the argument leading to (2.12), we find that the exponent λ characterizing the growth of the number of covering intervals satisfies the equation

$$\lambda^{N+n} - \lambda^{n-1} - \lambda^{n-2} \dots - \lambda - 1 = 0 \quad (3.13)$$

and ϵ satisfies

$$\epsilon^{N+1} + \epsilon^{N+2} + \dots + \epsilon^{N+n} = \frac{1}{n} \quad (3.14)$$

in order that the sum of the bandwidths is $1/n$ to mimic the Thouless property. Summing the geometric series in (3.13) and (3.14), making the substitutions

$$\lambda = n^{(1+\xi_1)/(N+n)}, \quad \epsilon = n^{-(2+\xi_2)/(N+n)} \quad (3.15)$$

and expanding the small parameters ξ_1 and ξ_2 in powers of $y = (N+n)^{-1}$, we find, after some algebra

$$\begin{aligned} \log_e \lambda &= y \log_e n \{ 1 + \frac{1}{2}(n-1)y + \frac{1}{24}[(n^2-1) \log_e n \\ &\quad + 6(n-1)^2 y^2] \} + O(y^3), \\ \log_e \epsilon &= -y \log_e n \{ 2 + (n-1)y + \frac{1}{6}[(n^2-1) \log_e n \\ &\quad + 3(n-1)^2 y^2] \} + O(y^3). \end{aligned} \quad (3.16)$$

From these results we deduce that the box-counting dimension D_0 is

$$D_0 = \frac{1}{2} - \frac{(n^2-1) \log_e n}{48(N+n)^2} + O(N^{-3}). \quad (3.17)$$

For the specific model we considered above, we have

$$\mu_1 = [N + \frac{1}{2}(n+1)] \log_e \epsilon, \quad \sigma_1^2 = \frac{1}{12}(n^2-1) \log_e^2 \epsilon. \quad (3.18)$$

Substituting the value of σ_1^2 for our specific model, given in (3.18), we find that (3.11) gives a result that is in agreement with the more rigorous result (3.17).

IV. A MODEL FOR THE SPREAD OF A WAVE PACKET

In this section, we describe a simplified model for the spread of a wave packet, based on the semiclassical analysis given in Refs. 14 and 15. This semiclassical analysis assumes that all of the continued fraction coefficients are large, and to avoid irrelevant complications we consider only the case where β is a quadratic irrational with continued fraction expansion $\beta = [n, n, n, \dots]$, with $n \gg 1$.

According to the simplest semiclassical picture, the spectrum and dynamics are determined by the contours of a classical Hamiltonian function $H(x, p) = 2(\cos x + \cos p)$. Because the contours of the classical Hamiltonian function are closed curves, the spectrum is predicted to be discrete, and the energy levels can be obtained from Bohr-Sommerfeld quantization. The spread of the wave packet is determined by classical motion along contours of this Hamiltonian: it spreads ballistically ($x \sim t$) until the spatial extent of the wave packet is $\Delta x = O(1)$, and it then stops spreading.

The more refined semiclassical analysis discussed in Ref. 15 considers the effect of tunneling between contours of the classical Hamiltonian. The tunneling effect broadens each of the n discrete levels predicted by Bohr-Sommerfeld quantization into a narrow band of width $8\Delta E_j$, where ΔE_j is a matrix element determined by the semiclassical approximation (2.3). The structure of each band is described by a renormalized Hamiltonian of the approximate form $H(x', p') \sim 2\Delta E_j(\cos x' + \cos p')$ similar to the original one. The length scale is expanded by a factor of $1/\beta$, i.e., $x' = \beta x$, and the time scale of the dynamics is expanded by a factor of $1/\Delta E_j$. That component of the original wave packet which excites the j th level therefore subsequently spreads ballistically, with velocity $v \sim \Delta E_j/\beta$, until its extent is $\Delta x = O(1/\beta)$. Because the renormalized Hamiltonian is similar in form to the original one, this line of argument can be repeated indefinitely, provided that the semiclassical condition $\beta \ll 1$ is also satisfied for the renormalized Hamiltonian.

Now consider the implications of this picture for the spread of a wave packet under the false assumption that all of the bandwidths ΔE_j are equal. Thouless's scaling law (2.1) would imply that the width of each of the n bands is C/n^2 . According to the discussion above, the wave packet would, therefore, undergo periods of ballistic growth, the first with velocity $v \sim 1$ until $\Delta x \sim 1$, then with velocity $v \sim n\Delta E \sim 1/n$, until $\Delta x \sim n$, etc. In general there would be periods during which the wave packet spreads with velocity $v \sim 1/n^k$, until the extent

of the wave packet is $\Delta x \sim n^k$. Figure 2(a) illustrates schematically the growth of the second moment implied by this picture, with periods of ballistic spreading punctuated by intervals of slower growth. The average rate of spreading implied by this picture is clearly diffusive, in the sense that

$$\gamma_2 = \lim_{t \rightarrow \infty} \left[\frac{\log_e \langle x^2 \rangle}{\log_e t} \right] = 1, \quad (4.1)$$

but there are large fluctuations that are more marked in the limit $n \rightarrow \infty$. According to this model, the growth of the N th moment is $\langle x^N \rangle \sim t^{N/2}$.

It is necessary to consider how this picture will change when we take into account the fact that not all of the bands have the same width. Components of the wave packet associated with different bands will spread with different velocities, and the episodic spread indicated in Fig. 2(a) would be expected to be replaced by a smoother growth for sufficiently large times, as illustrated in Fig. 2(b). Semiclassical arguments²⁰ indicate that most of the n bands are exponentially small, and that most of the total bandwidth $1/n$ is shared between a set of $\sim \log_e n$ bands of typical width $\sim 1/n \log_e n$. We assume that the probability p for the electron to be in a given band is the same for the large bands as for the exponentially small ones: $p \sim 1/n$.

The model of the spread of the wave packet must now be modified as follows. The wave packet initially spreads ballistically with velocity $v \sim 1$ until $\Delta x \sim 1$. A fraction $P \sim \log_e n/n$ of the wave packet subsequently undergoes ballistic spread with velocity $v \sim n \Delta E_{\max} \sim 1/\log_e n$, (where ΔE_{\max} is the width of the widest band) until $\Delta x \sim n$. The remainder, associated with the very narrow bands, spreads much more slowly. In general, the fastest spreading component of the wave packet reaches $\Delta x \sim n^k$ with velocity $v \sim (\log_e n)^k$ at time $t \sim (n \log_e n)^k$. The proportion of wide bands, of width $\Delta E_{\max} \sim (n \log_e n)^{-k}$ is $P \sim (\log_e n/n)^k$. These bands dominate the N th moment of the wave packet, which therefore has value

$$\langle x^N \rangle \sim P x^N \sim (\log_e n)^k n^{(N-1)k}, \quad (4.2)$$

when

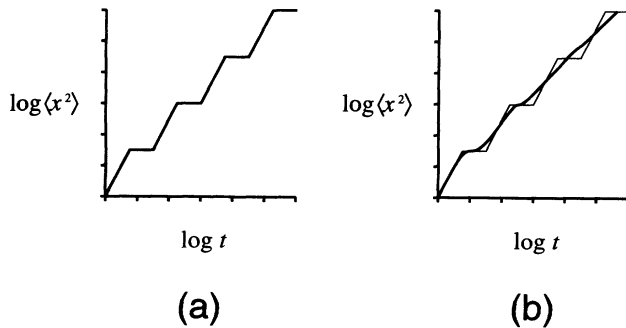


FIG. 2. Schematic illustration of growth of second moment of wave packet. (a) Episodic growth predicted if spectrum is exactly self-similar. (b) If there is dispersion in the widths of the bands, the steps are smoothed out.

$$t \sim 1/\Delta E \sim (n \log_e n)^k. \quad (4.3)$$

The predictions of this heuristic analysis can be summarized as follows. Comparing (4.2) and (4.3), we see that the second moment is still predicted to grow diffusively (i.e., $\gamma_2 = 1$) in the limit $n \rightarrow \infty$. The dynamics is, however, very different from a true diffusive process, in that components of the wave packet associated with the widest bands are spreading ballistically, whereas those associated with the exponentially narrow bands spread extremely slowly.

The difference between this behavior and standard diffusion is revealed by considering the higher moments. In a random diffusive process, the growth of the higher moments is $\gamma_N = N/2$. From (4.2) and (4.3), we see that the model implies a different prediction for the exponents γ_N :

$$\gamma_N = \lim_{t \rightarrow \infty} \frac{\log_e \langle |x^N| \rangle}{\log_e t} \sim (N-1) - \frac{(N-2) \log_e (\log_e n)}{\log_e n + \log_e (\log_e n)}. \quad (4.4)$$

Thus, in the limit $n \rightarrow \infty$, this model predicts that the exponents γ_N approach $(N-1)$ very slowly, with corrections which are logarithmic in $\log_e n$. We emphasize that this is just a heuristic model, and not (for example) the leading order asymptotic behavior in the limit $n \rightarrow \infty$.

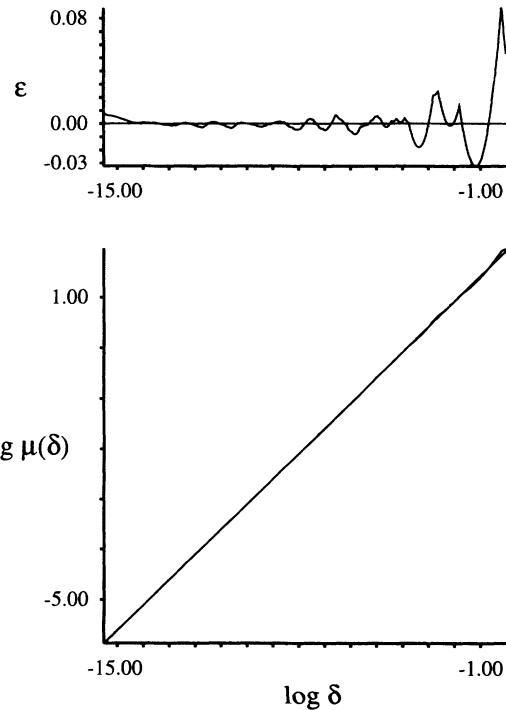


FIG. 3. Logarithmic plots of the measure $\mu(\delta)$ of the delta parallel body versus δ , for four rational approximants to $\beta = [1, 1, 1, \dots]$, together with a least squares fit. The upper plot is the error of the least squares fit, for the largest denominator. Logarithms are in base e here and throughout the figures.

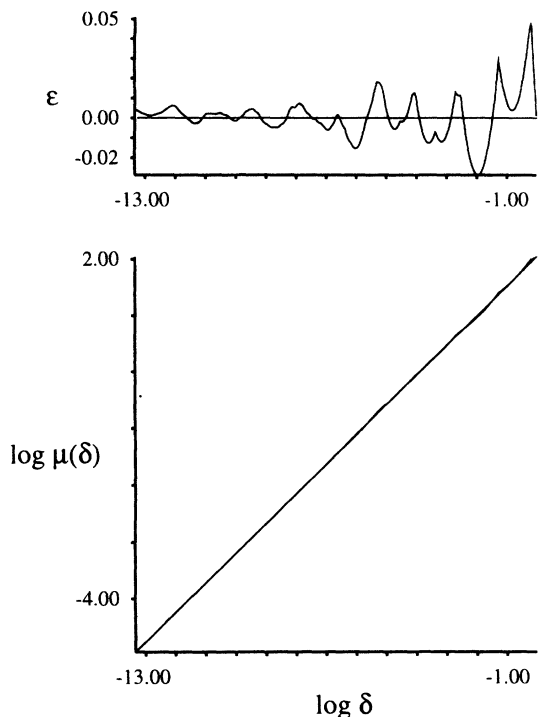


FIG. 4. Same as Fig. 3, for a single rational approximant to $\beta = [4, 4, 4, \dots]$.

V. NUMERICAL RESULTS

A. Dimension of the spectrum

We estimated the box-counting dimension numerically using a sequence of rational approximants p_i/q_i to the desired irrational β . Rather than using the direct technique of counting the minimal number of intervals required to cover the set, we used a slightly different approach that is easier to program. We computed the measure $\mu(\delta)$ of the δ parallel body of the spectrum: this is the set of points within a distance δ of at least one point in the spectrum. The box-counting dimension is related to $\mu(\delta)$ as follows:⁵

$$1 - D_0 = \lim_{\delta \rightarrow 0} \frac{\log_e[\mu(\delta)]}{\log_e \delta}. \tag{5.1}$$

TABLE I. Box-counting dimensions D_0 , bandwidth distribution parameters μ_1 and σ_1^2 , and growth exponents γ_N for quadratic irrationals of the form $\beta = [n, n, n, \dots]$, together with an estimate D_0^{th} of D_0 obtained from (3.11).

n	D_0	μ_1	σ_1^2	γ_2	γ_4	γ_6	D_0^{th}
1	0.498	-0.97	0.0184	0.95	1.93	2.95	0.498
2	0.493	-1.81	0.0774	0.92	1.88	2.96	0.495
3	0.486	-2.52	0.257	0.84	1.84	2.96	0.487
4	0.476	-3.17	0.623	0.87	2.06	3.34	0.473
5	0.468	-3.78	1.201	0.91	2.21	3.52	0.454
10				0.94	2.29	3.67	
15				0.99	2.35	3.73	

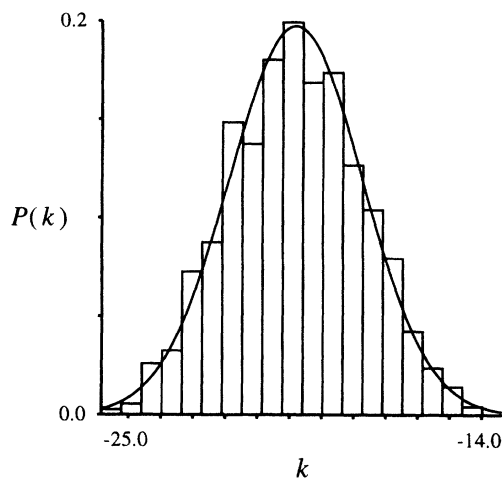


FIG. 5. Histogram of the distribution of logarithms k of the bandwidths, for $\beta = 5473/23184$, an approximant of $[4, 4, 4, \dots]$, showing that these are approximately log-normal distributed.

In Fig. 3(a), we plot $\log_e \mu(\delta)$ against $\log_e \delta$ for a sequence of principal approximants to various irrational values of $\beta = [1, 1, 1, \dots]$, the largest denominator being 17711. The curves follow the same straight line until δ becomes smaller than the largest band; this is strong evidence that the box-counting dimension exists and that it can be approximated using these data. A least squares fit to this line gives a box-counting dimension of $D_0 \approx 0.498$. It is not meaningful to give an error estimate, because the deviations from the straight line are not random. The deviation is plotted in Fig. 3(b), showing decreasing oscillations, which would be predicted from the arguments above. In Fig. 4, we plot data for $\beta = [4, 4, 4, \dots]$, for a single approximant $p/q = 5473/23184$. Here we see that the deviations from a straight line are more pronounced. Values of D_0 are listed in Table I for various n ; they are all less than one half, and decrease slowly as n increases.

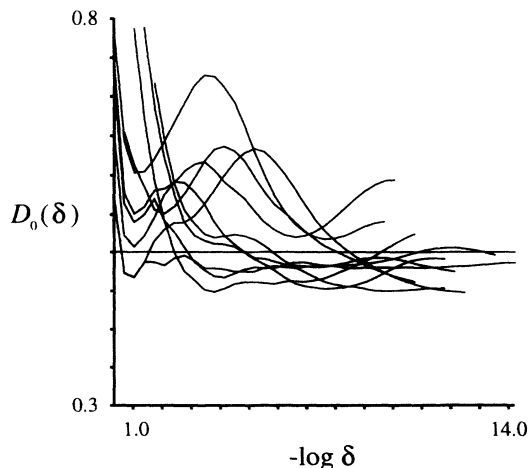


FIG. 6. Plot of approximate dimension D_0 versus δ for ten approximants to random irrationals.

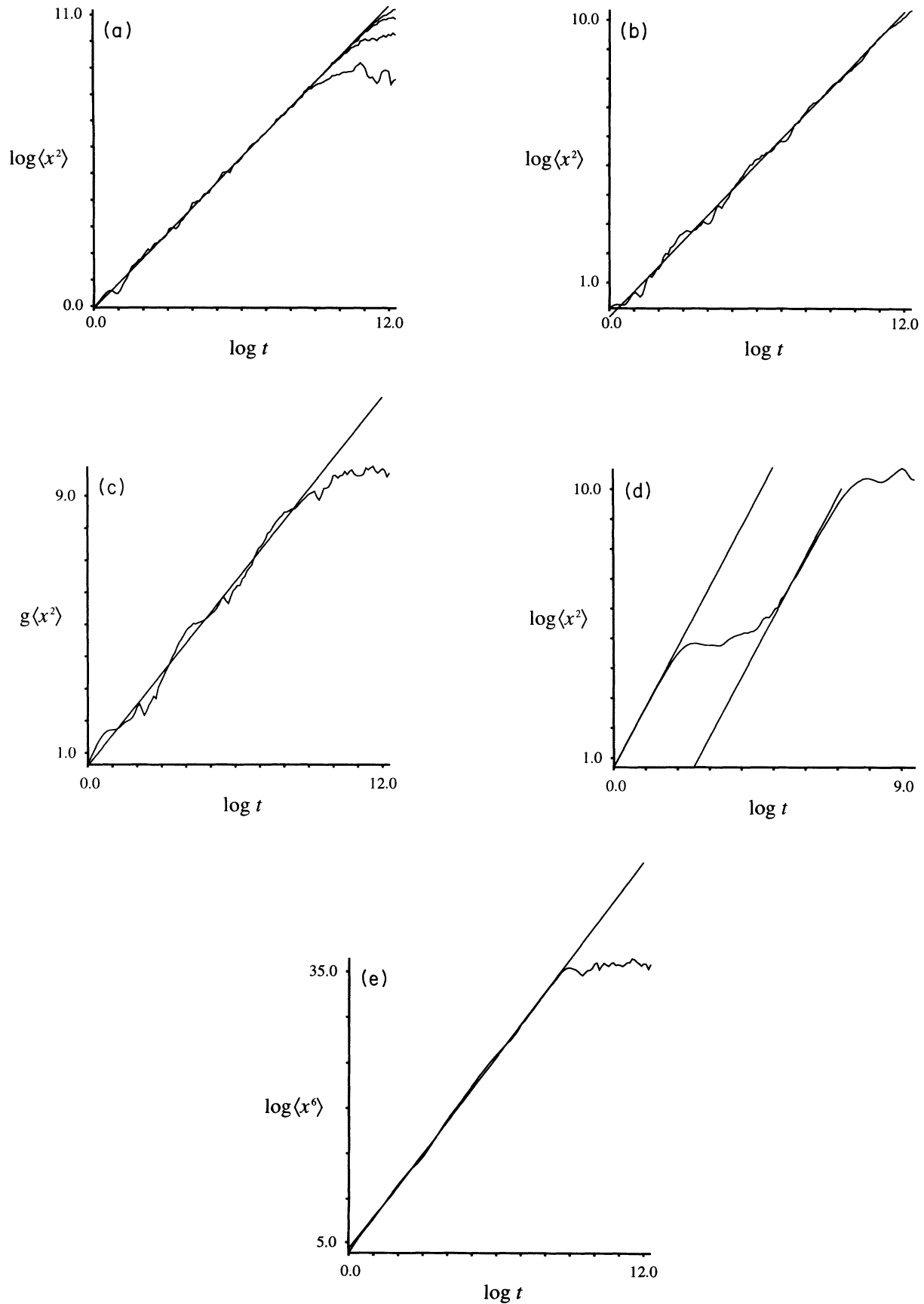


FIG. 7. Logarithmic plot of the moments of an initially localized wave packet versus time, for $\beta = [n, n, n, \dots]$. (a)–(d) are plots of $\langle x^2 \rangle$, with $n = 1, 3, 10, 50$; (e) is $\langle x^6 \rangle$, for $n = 10$.

The model described in Secs. II and III suggests that the bandwidths of a rational approximant should be log-normal distributed. Figure 5 is a histogram of the logarithms of the bandwidths for the same data as used in Fig. 4. The graph shows a normal distribution for comparison, with the same mean and variance as the logarithms of the bandwidths. The model of Sec. III also predicts that the mean and variance of the distribution should be linearly dependent on the order k of the rational approximant:

$$\mu = \mu_0 + k\mu_1, \quad \sigma^2 = \sigma_0^2 + k\sigma_1^2. \quad (5.2)$$

This expectation is confirmed with high accuracy, and in Table I we also list the coefficients μ_1 and σ_1^2 : note that σ_1^2 increases with n , in agreement with the prediction that the dispersion in the sizes of the bands should be larger in the semiclassical limit.

In Table I we also list “theoretical” values of the box-counting dimension obtained from (3.11), using the empirical values for the constant σ_1^2 given in this table, and substituting $1/\beta$ for the constant \tilde{n} . The values are in quite close agreement with the numerically computed dimension for smaller values of n .

In Fig. 6 we show data on the fractal dimension for ten randomly chosen numbers. We chose large-order rational approximants, and plotted the approximate dimension

$$D_0 = 1 - \frac{\log_e[\lambda\mu(\delta)]}{\log_e \delta} \quad (5.3)$$

(where λ is a constant) as a function of $\log_e \delta$, for values of δ down to the size of the largest band. The value of λ was chosen to give the best approximation to a straight line. The results are far from conclusive, but these data are not inconsistent with the hypothesis that the box-counting dimension exists and converges to the same value for almost all β , and that its value is slightly less than one-half. It is difficult to extend these calculations to higher rational approximants because of numerical difficulties in identifying the band edges accurately for denominators q greater than 3×10^4 .

B. Spread of an initially localized wave packet

We performed some numerical experiments on the spread of a state that was initially localized at the $n = 0$ site, i.e., $\psi_n(0) = \delta_{n0}$. The solution of the time dependent Schrödinger equation was computed numerically for a finite-sized lattice, first by computing the eigenfunctions by matrix diagonalization, and secondly (as a check) by integration using fourth-order Runge-Kutta. The parameter θ in (1.1) was set to zero in all of our numerical calculations. We characterized the spread of the wave packet by calculating moments defined by (1.2).

We show some results for the second moment in Figs. 7(a)–(d) for four different $\beta = [n, n, n, \dots]$. The graphs for $n = 1, 3, 10$ show least squares fits of a linear function for comparison, and the slopes γ_2 are listed in Table I. Figure 6(a) shows the saturation occurring at different times due to three different finite basis sizes (the largest

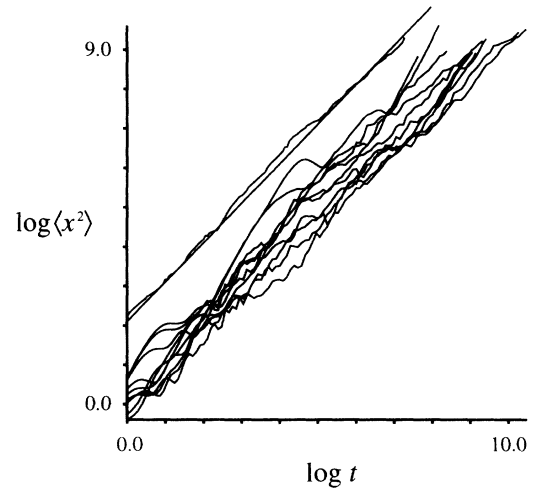


FIG. 8. Plot of $\langle x^2 \rangle$ for ten random irrational values of β . An averaged curve is also plotted, shifted vertically from the others, with a line of unit slope for comparison.

being 2000). The graph for $n = 50$ shows the intervals of ballistic growth predicted in Sec. IV; the straight lines have a slope of 2, corresponding to ballistic motion, and their vertical offset is 5.01, which is close to the value $\log_e(n \log_e n) = 5.28$ predicted by the heuristic model.

Figure 7(e) shows the growth of the sixth moment for $n = 10$, together with a straight line fit. The data for the higher moments showed smaller fluctuations than the lower moments. The exponents for the higher moments are listed in Table I. In the limit $n \rightarrow \infty$ they are higher than those predicted by the oversimplified model which ignores the dispersion of the band sizes, and as $n \rightarrow \infty$ they appear to approach the limiting values $N - 1$ predicted in Sec. IV. The predictions of (4.4) for $n = 15$ are $\gamma_2 = 1$, $\gamma_4 = 2.47$, and $\gamma_6 = 3.96$, which are in reasonable agreement with the data in Table I.

In Fig. 8, we have plotted the second moment for ten randomly chosen irrationals. The mean of the ten values of $\log_e \langle x^2 \rangle$ is also plotted; this curve was shifted vertically for clarity, and a straight line of slope unity has been superposed for comparison. The data suggest that the growth may be asymptotically a power law with an exponent close to unity.

VI. CONCLUDING REMARKS

Our numerical results and heuristic arguments indicate that neither of the proposed relationships $D_0 = \frac{1}{2}$ or $\gamma_2 = 2D_0$ are exactly correct. We have argued, using a combination of Thouless’s result²⁰ on the bandwidth of rational approximants and a renormalization group approach, that both of these relationships would be valid if all of the subbands of the hierarchical division of the spectrum were identical. In practice, this assumption is not valid, primarily because the bandwidths can be very different.

We have presented heuristic arguments for the class of quadratic irrationals of the form $\beta = [n, n, n, \dots]$, which

indicate that the dispersion of the bandwidths increases as $n \rightarrow \infty$, and that $D_0 \rightarrow 0$ in this limit, whereas $\gamma_2 \rightarrow 1$. These arguments would indicate that there are not any generally applicable equalities relating any of the generalized dimensions to the dynamics.

Our numerical results confirm the predictions that the dispersion of the bandwidths increases as $n \rightarrow \infty$. Our heuristic model for the dimension of the spectrum is in quite good agreement with the numerical values for small n , which show that $D_0 < \frac{1}{2}$ and that it decreases as $n \rightarrow \infty$. Our results for the growth exponents are in qualitative agreement with a model that indicates that $\gamma_N \sim N/2$ when the dispersion coefficient of the band-

widths σ_1^2 is small at $n = 1$, crossing over to $\gamma_N \sim N - 1$ in the limit $n \rightarrow \infty$.

ACKNOWLEDGMENTS

We benefited from stimulating discussions with Professor J. Avron and Professor S. Fishman, and particularly Dr. Yoram Last. We acknowledge support from the quantum chaos program at the Institute of Theoretical Physics, Technion and are grateful for hospitality during our visit there. This work was also supported by the U.K. Science and Engineering Research Council.

* Present address: Laboratoire de Physique Quantique, Université Paul Sabatier, 118 Route de Narbonne, F-31062 Toulouse Cédex, France.

† Permanent address: Department of Physics and Applied Physics, John Anderson Building, University of Strathclyde, Glasgow G4 0NG, Scotland, United Kingdom.

¹ R. Peierls, *Z. Phys.* **80**, 763 (1933).

² P. G. Harper, *Proc. Phys. Soc. London Sect. A* **68**, 879 (1955).

³ A. Rauh, *Phys. Status Solidi B* **65**, 131 (1974).

⁴ A. Rauh, *Phys. Status Solidi B* **69**, 9 (1975).

⁵ K. J. Falconer, *Fractal Geometry: Mathematical Foundations and Applications* (Wiley, New York, 1990).

⁶ I. Guarneri, *Europhys. Lett.* **10**, 95 (1989).

⁷ I. Guarneri, *Europhys. Lett.* **21**, 729 (1993).

⁸ T. Geisel, R. Ketzmerick, and G. Petschel, *Phys. Rev. Lett.* **66**, 1651 (1991).

⁹ R. Ketzmerick, G. Petschel, and T. Geisel, *Phys. Rev. Lett.* **69**, 695 (1992).

¹⁰ I. Guarneri and G. Mantica, *Ann. Inst. H. Poincaré* (to be

published).

¹¹ C. Tang and M. Kohmoto, *Phys. Rev. B* **34**, 2041 (1986).

¹² J. Bell and R. B. Stinchcombe, *J. Phys. A* **20**, L739 (1987).

¹³ M. Ya. Azbel, *Zh. Eksp. Teor. Fiz.* **46**, 929 (1964) [*Sov. Phys. JETP* **19**, 634 (1964)].

¹⁴ I. M. Suslov, *Zh. Eksp. Teor. Fiz.* **83**, 1079 (1982) [*Sov. Phys. JETP* **56**, 612 (1982)].

¹⁵ M. Wilkinson, *Proc. R. Soc. London Ser. A* **391**, 305 (1984).

¹⁶ D. R. Hofstadter, *Phys. Rev. B* **14**, 2239 (1976).

¹⁷ M. Wilkinson, *J. Phys. A* **20**, 4337 (1987).

¹⁸ Y. Last, *Commun. Math. Phys.* (to be published).

¹⁹ D. J. Thouless, *Phys. Rev. B* **28**, 4272 (1983).

²⁰ D. J. Thouless, *Commun. Math. Phys.* **127**, 187 (1990).

²¹ Y. Last and M. Wilkinson, *J. Phys. A* **25**, 6123 (1992).

²² J. Avron, P. H. M. van Mouche, and B. Simon, *Commun. Math. Phys.* **132**, 103 (1990).

²³ M. Kac, *Carus Mathematical Monographs* No. 12 (Mathematical Association of America, Oberlin, OH, 1959).

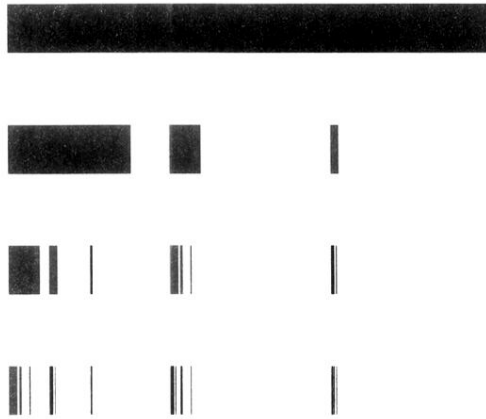


FIG. 1. Illustrating four stages of the construction of the model Cantor set for $n = 3$.